Jewitt (7). If the material is primarily icy grains, then the dust fluxes calculated by these authors must be increased (because the grains sublime slowly, even at these distances) and we would require more frequent outbursts, but they would still be consistent with the variability seen in the photometric measurements of Chiron (7, 16, 23). Our steady-state scenario also provides a mass of grains more than sufficient to replenish the grains as cited by the aforementioned authors. We believe that the photometric variability is the strongest argument in favor of the outburst over the steady-state scenario; this is dramatically confirmed by the recent announcement by Cochran and Cochran (24) that the upper limit on the abundance of CN a month before our observations was a factor of 2 lower than our measured value.

The next significant question is whether the outgassing is driven by CO or by CO_2. CO was much more abundant in P/Halley than was CO_2 but a large fraction (at least half, possibly all) of the CO came from a distributed source which could not be responsible for driving the outburst whereas CO_2 was a parent molecule (20, 22). Furthermore, CO_2 seems omnipresent in comets (based on observations of CO_2^+) whereas CO appears to vary drastically from one comet to another (25). Meech and Belton (16) chose CO in their model because it provided a higher mass-flux with which to lift grains from the surface. Because the flux of the two species differs by less than an order of magnitude for our assumed parameters of the ice, and because the lift-off of grains depends very strongly on the size-to-mass ratio of the grains, we think that the much stronger argument derives from the variability. At this heliocentric distance (11.3 AU), the vaporization of CO_2 would be at a temperature near 94 K and very sensitive to the incident insolation whereas the vaporization of CO would be at a temperature near 34 K and vary linearly with insolation; in other words, this is the "turn-on" distance for CO_2 (19). Thus pockets of CO_2 ice slightly below the surface are just reaching the temperature at which they vaporize and can drive outbursts whereas any such pockets of CO would likely have vaporized at larger heliocentric distances unless they are much deeper below the surface of the nucleus. Presumably the overall brightness surge in 1988–1990 is attributable to the accumulated coma of grains from many of these smaller outbursts. We note that Stern (10) has made some of these same points in a slightly different context.

Finally, it is also worth pointing out that outgassing from a small fraction of the surface of a comet's nucleus appears to be a characteristic of comets that have made many passages close to the sun (18), but somewhat less characteristic of comets that have not undergone many close passages. Is the localization of activity on Chiron therefore a sign of chemical heterogeneity? If so, it would indicate that cometary nuclei accreted from smaller lumps that condensed at different locations in the solar nebula.

REFERENCES AND NOTES

1. C. T. Kowal, in *Asteroids*, T. Gehrels, Ed. (Univ. of Arizona Press, Tucson, 1979), pp. 436–439.
2. S. Oikawa and E. Everhart, *Astron. J.* **84**, 134 (1979); H. Scholl, *Icarus* **40**, 345 (1979); C. T. Kowal, W. Liller, B. G. Marsden, in *Dynamics of the Solar System*, R. L. Duncombe, Ed. (Reidel, Dordrecht, 1979), pp. 245–250.
3. W. K. Hartmann, D. P. Cruikshank, J. Degewij, R. W. Capps, *Icarus* **47**, 333 (1981); L. A. Lebofsky, D. J. Tholen, G. H. Rieke, M. J. Lebofsky, *ibid.* **60**, 532 (1984); B. Zellner, D. J. Tholen, E. F. Tedesco, *ibid.* **61**, 355 (1985).
4. D. J. Tholen, W. K. Hartmann, D. P. Cruikshank, *Int. Astron. Union Circ. 4554*, 24 February 1988; S. J. Bus, E. Bowell, A. W. Harris, A. V. Hewitt, *Icarus* 77, 223 (1989).
5. K. J. Meech and M. J. S. Belton, *IAU Circ.* No. 4770, 11 April 1989.
6. R. M. West, *The Messenger*, No. 60, 57 (1990).
7. J. X. Luu and D. C. Jewitt, *Astron. J.* **100**, 913 (1990).
8. W. K. Hartmann *et al.*, *Icarus* **83**, 1 (1990).
9. W. D. Cochran, A. L. Cochran, E. S. Barker, in *Asteroids, Comets, Meteorites II*, C.-I. Lagerkvist, B. A. Lindblad, H. Lundstedt, H. Rickman, Eds. (Uppsala University, Sweden, 1986), pp. 181–185.
10. S. A. Stern, *Pub. Astron. Soc. Pacific* **101**, 126 (1989).
11. D. G. Schleicher, thesis, University of Maryland (1983).
12. F. P. Schloerb, W. M. Kinzel, D. A. Swade, W. M. Irvine, *Astron. Astrophys.* **187**, 475 (1987).
13. M. F. A'Hearn *et al.*, *Nature* **324**, 649 (1986).
14. J. Crovisier and D. Bockelée-Morvan, in *Asteroids, Comets, Meteorites II*, C.-I. Lagerkvist, B. A. Lindblad, H. Lundstedt, H. Rickman, Eds. (Uppsala University, Sweden, 1986), pp. 289–292.
15. M. C. Festou, *Astron. Astrophys.* **95**, 69 (1981).
16. K. J. Meech and M. J. S. Belton, *Astron. J.* **100**, 1323 (1990).
17. M. V. Sykes and R. G. Walker, *Science* **251**, 777 (1991).
18. M. F. A'Hearn, in *Annu. Rev. Earth Planet. Sci.* **16**, pp. 273–293 (1988); P. R. Weissman, M. F. A'Hearn, L. A. McFadden, H. Rickman, in *Asteroids II*, R. P. Binzel, T. Gehrels, M. S. Matthews, Eds. (Univ. of Arizona Press, Tucson, 1989), pp. 880–920.
19. J. J. Cowan and M. F. A'Hearn, *Icarus* **50**, 53 (1982).
20. V. I. Moroz *et al.*, *Astron. Astrophys.* **187**, 513 (1987).
21. D. G. Schleicher *et al.*, in *20th ESLAB Symposium on the Exploration of Halley's Comet, ESA SP-250*, (European Space Agency, Heidelberg, 1986), vol. 1, p. 565.
22. P. Eberhardt *et al.*, *Astron. Astrophys.* **187**, 481 (1987).
23. B. J. Buratti and R. S. Dunbar, *Astrophys. J.* **366**, L47 (1991).
24. W. Cochran and A. Cochran, *Int. Astron. Union Circ. 5144*, 12 December 1990.
25. P. D. Feldman, *Science* **219**, 347 (1983).

26. We gratefully thank B. L. Lutz, R. M. Wagner, and S. A. Stern for their suggestions and encouragement throughout this project. We also thank R. Bertram for his tireless assistance in obtaining the observations. This work is supported by NASA grant NAGW-1470 (for S.J.B. and E.B.), NASA grant NAGW-1864 (for D.G.S.), NASA grant NAGW-1886 (for M.F.A.) and from the Lowell Observatory endowment.

5 October 1990; accepted 2 January 1991

Constraints on the Diameter and Albedo of 2060 Chiron

Mark V. Sykes and Russell G. Walker

Asteroid 2060 Chiron is the largest known object exhibiting cometary activity. Radiometric observations made in 1983 from a ground-based telescope and the Infrared Astronomical Satellite are used to examine the limits on Chiron's diameter and albedo. It is argued that Chiron's surface temperature distribution at that time is best described by an "isothermal latitude" or "rapid-rotator" model. Consequently, Chiron has a maximum diameter of 372 kilometers and a minimum geometric albedo of 2.7%. This is much bigger and darker than previous estimates, and suggests that gravity may play a significant role in the evolution of gas and dust emissions. It is also found that for large obliquities, surface temperatures can vary dramatically on time scales of a decade, and that such geometry may play a critical role in explaining Chiron's observed photometric behavior since its discovery in 1977.

Chiron has elicited considerable interest since its discovery in 1977 as the most distant known asteroid (1, 2). Most asteroids reside between the orbits of Mars (at 1.5 AU) and Jupiter (at 5.2 AU). Chiron ranges between 8.5 and 19 AU from the sun, crossing the orbit of Saturn. Since 1987, Chiron has been exhibiting non-asteroidal behavior, increasing in brightness more than would be expected for an airless body approaching the sun (3). Cometary activity was suspected (4–7), but no coma was seen until 1989, when it was detected in a deep CCD image by Meech and Belton (8). 2060 Chiron thus

M. V. Sykes, Steward Observatory, University of Arizona, Tucson, AZ 85721.
R. G. Walker, Jamieson Science and Engineering, Inc., 5321 Scotts Valley Drive, Scotts Valley, CA 95066.

became the first numbered asteroid known to behave like a comet (*9*).

The surface temperature and gravitational field of Chiron are necessary to understanding the Chiron atmosphere and the photometric activity observed prior to the detection of the coma (*10*). Surface temperatures, dependent upon the subsolar latitude and properties such as the albedo, determine which molecular species may be driving the cometary activity of this object (*11*). Utilizing observations made by the Infrared Astronomical Satellite (IRAS) and earlier ground-based measurements, we derive constraints on the diameter and albedo of Chiron, and consider their dependence on different thermal models. The resulting surface temperatures and their implications for Chiron's recent activity are also discussed.

Observations at thermal infrared wavelengths from ground-based telescopes have shown several short-period comet nuclei to have diameters on the order of 10 km (*12–14*). This is similar in size to Comet Halley as seen by the Giotto and Vega spacecraft (*15, 16*). Comet nuclei have also been found to be very dark, with geometric albedos less than ~0.05 (*12–16*). In contrast, ground-based radiometry has inferred a nominal diameter of 180 km for Chiron and a corresponding albedo of 0.10 (*17*), making it the largest known cometary body by an order of magnitude. This diameter may be too small.

The model used in determining the earlier values is referred to as the asteroid standard thermal model (STM). It presumes that the surface is a sphere in radiative equilibrium with incident sunlight. That is, the temperature is highest at the subsolar point, falling as $\cos^{1/4}\theta$ on the sunlit side, where θ is the angle between the subsolar point and the point of interest on the surface. The temperature on the dark side is assumed to be zero (*18*). For most asteroids this model is a good approximation. However, in the outer solar system, objects tend to lose heat from their thermal skin through radiation on time scales much longer than their rotation periods. In this situation the difference between daytime and nighttime temperatures is small, and a point on the surface achieves a temperature in radiative equilibrium with the average amount of sunlight it receives over a rotational period. This is referred to as the isothermal latitude (ILM) or "rapid-rotator" model (*18*), though the object actually may not be rotating rapidly. This breakdown of the STM for cold, distant objects has been modeled for comets (*19*) and Pluto (*20*), and has been generalized to other solar system objects (*21*).

The test to determine whether an object is characterized more accurately by the standard thermal model or an isothermal latitude model is the value of its thermal parameter, Θ, which is unitless and defined as

$$\Theta = \frac{\Gamma\sqrt{\varpi}}{\epsilon\sigma T^3} \qquad (1)$$

where Γ is the thermal inertia of the surface, ω is the angular rotation rate of the body, ϵ is the bolometric emissivity, σ is the Stephan-Boltzmann constant, and T is the subsolar equilibrium temperature for a nonrotating body given by

$$T = \left[\frac{(1 - A)F_{\odot}}{\epsilon\sigma R^2}\right]^{1/4} \qquad (2)$$

where A is the bolometric Bond albedo, $F_{\odot}$ is the solar constant, and R is the heliocentric distance in astronomical units (*21*). Values of Θ much less than unity indicate that the STM is a good approximation to the thermal behavior of an object, while values much greater than unity argue for the adoption of an isothermal latitude model. However, as the subsolar latitude increases, even a rapidly rotating body will look more like an STM because an increasing fraction of the surface is constantly illuminated. Finally, if the sun is shining directly down onto the rotational pole, the object will be indistinguishable from an STM regardless of its rotational rate or thermal inertia.

Radiometric observations of Chiron have been made twice, both in 1983. These consisted of ground-based observations (*17*), and observations by the Infrared Astronomical Satellite (IRAS). The observing circumstances are recorded in Table 1. A rotational period of ~7 hours, estimated by Lebofsky *et al.* (*17*), has been further refined to 5.9180 hours by Bus *et al.* (*6*). The thermal inertia of Chiron's surface is unknown. Ranges in the solar system (to date) vary from the asteroids Ceres and Pallas (~10^4 erg $cm^{-2}s^{-1/2}$ K^{-1}) (*21*) to the Jovian moon Ganymede (7×10^4 erg $cm^{-2}s^{-1/2}$ K^{-1}) (*22*). If we assume that Chiron's surface has an albedo of zero and unit emissivity (minimizing Θ), this range of thermal inertias yields values of Θ between 3 and 22. Increasing albedo and emissivity to values determined and used by Lebofsky *et al.* (*17*) will increase Θ by a few percent. These values suggest that Chiron is best modeled radiometrically as a rapidly rotating body if the subsolar point is near the equator.

We can constrain the plausible range of subsolar latitudes by noting that during 1983, Chiron exhibited a light curve at visual wavelengths with an amplitude determined tentatively (because of low signal to noise) by Lebofsky *et al.* (*17*) which corresponds to a change in projected surface area of 74% (assuming light curve variations caused solely by shape). Observations nearly 4 years later by Bus *et al.* (*6*) show a well-defined light curve with an amplitude corresponding to a change in projected surface area of 18%. Comets are thought to be fairly elongated objects having axial ratios ranging up to ~2:1 (*23*). Planetary satellites that are as large as Chiron are much more spherical, possibly as a consequence of gravity (*24*). However, for the sake of argument, if we assume Chiron to have such an extremely elongated shape, and further assume its surface to be an isotropic scatterer, then the light curve variations seen by Lebofsky *et al.* would require a subsolar latitude of 20°. The Bus *et al.* amplitude would correspond to a subsolar latitude of 53° (*25*). When the subsolar latitude is less than 30°, departure from ILM is small when Θ is large (*21*). Around subsolar latitudes of 60°, we are well within the transition region between ILM and STM. In the above calculations, as we decrease the elongation of Chiron's shape, the subsolar latitudes are driven closer to the equator, further arguing for the isothermal latitude model. A light curve can also result from albedo variations across a surface, however, and can either enhance or counter the effects of shape. Thus, while the standard thermal model cannot be ruled out for Chiron at the time of the radiometric observations, the isothermal latitude model appears to offer the more reasonable description of its surface, based on what little information we possess. Both models will be considered in this work.

The position of Chiron was scanned twice by IRAS. Two detectors in each wavelength band (*26*) passed over Chiron on each scan, giving a total of four scans per band. The four scans were transformed to the Chiron centered coordinate system, the fluxes averaged (with inverse invariance weighting), and the resulting coadded data passed through the IRAS zero-sum point source detection filter (*26*). Structures near the location of Chiron are reproduced at both 60 and 100 μm and have radiance ratios characteristic of infrared cirrus. No source

Table 1. Observation circumstances and model parameters.

Source	Ground-based (*17*)	IRAS
Date (1983)	Jan 9/10	Sep 16
Heliocentric distance (AU)	15.72	15.36
Geocentric distance (AU)	15.15	14.99
Solar phase angle (°)	2.98	3.53
Derived quantities		
H_V (*31*)	6.7	
G (*31*)	0.7	
β_E (mag/degree) (*31*)	0.01	
η (ILM) (*31*)	1.0	
η (STM) (*31*)	0.756	
ϵ (*18*)	0.9	

was detected at the position of Chiron with flux greater than 1.4 times the standard deviation of the signal measured at the filter output. The 3σ detection limits based on this measure of the noise for the 25 and 60 μm bands are 80 and 135 mJy, respectively, and are adopted as the upper bounds for flux from Chiron. The noise at 100 μm, which is dominated by the background clutter of infrared cirrus, is about an order of magnitude higher than that at 60 μm and thus does not significantly constrain the object's diameter or albedo. The 12-μm observations are similarly unconstraining since they are well on the Wien side of the blackbody emission of a body as cold as Chiron.

The ground-based observations by Lebofsky *et al.* (*17*) reported a detection of Chiron at the 1.9σ level of noise using a "narrow-*Q*" filter (*27*). We consider the possibilities that this may have been either a detection or noise excursion in constraining the diameter and albedo in our different models. In the latter case, we use 27 mJy at 22.5 μm as the 3σ measure of their reported noise.

Following the procedure outlined by Lebofsky and Spencer (*18*), and using the photometric parameters listed in Table 1, we calculated diameters and geometric albedos for the ILM and STM cases (Fig. 1). Regardless of the thermal model adopted, the relationship between the diameter and albedo is fixed by the absolute magnitude (*28*). The radiometry allows us to determine where on this curve the diameter and albedo lie. In the STM case, where the subsolar latitude is polar, the ground-based observations of Lebofsky *et al.* define the maximum diameter and minimum albedo of Chiron. If the detection at 22.5 μm is taken at face value, this corresponds to a diameter of 167 km and a geometric albedo of 0.136 (*29*). The subsolar temperature would be 107 K. If we consider the ground-based observation to have yielded an upper limit and not a detection, then the diameter would be less than 204 km, and the albedo larger than 0.091. This yields a subsolar temperature less than 108 K. In the ILM case, where the subsolar latitude is equatorial, the IRAS 60 μm upper limit is most constraining, resulting in a diameter less than 372 km, and an albedo greater than 0.027. This is as much as twice the Lebofsky *et al.* detection diameter (*17*), and one-quarter the albedo. The equatorial temperature would be less than 77 K. We believe this last case (ILM) provides the best limits on these parameters for Chiron.

The low-albedo limit of a few percent allows for the taxonomic identification of Chiron as a C-type asteroid, based on the colorimetric similarities at visual and near-infrared wavelengths pointed out by Hartmann *et al.* (*7*), and the fact that C-type asteroids are, on average, quite dark (*30*). Because Chiron, however, is an object which likely formed in the outer solar system, far removed from the main asteroid belt, it is not likely that it has the same composition as its taxonomic siblings. This should serve as a warning against automatically assuming compositional similarity even among main-belt asteroids of the same taxonomic class.

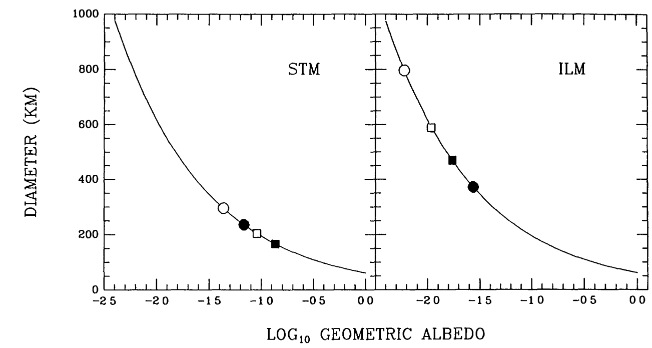

Fig. 1. Possible values and limits for the diameter and albedo of Chiron are shown assuming the surface temperature distribution is described by the standard thermal model (STM) or the isothermal latitude model (ILM). The curve in each case is defined by the absolute magnitude of Chiron (Table 1). Diameter and albedo in the STM are constrained most by ground-based observations at 22.5 μm (*17*) indicating either a 1.9σ detection (■), or a 3σ upper limit (□). Constraints are also shown for IRAS observations setting 3σ upper limits at 25 μm (○) and 60 μm (●). The latter defines the maximum diameter and minimum albedo in the ILM. In the case of upper limits, the true diameter and albedo of Chiron may fall anywhere to the right on the curve, that is, Chiron can be smaller and brighter.

The effect of gravity on gas outflow was estimated by calculating the fraction of molecules coming off the surface with speeds exceeding the escape velocity of Chiron assuming a mass density ρ = 1 g/cm^3 for the asteroid. The gas molecules (with the molecular weight of carbon monoxide) were assumed to have a Maxwell-Boltzmann speed distribution for a kinetic temperature equal to the equatorial surface temperature in the ILM case, and the subsolar temperature in the STM case. Sublimation would result in a decreased surface temperature, hence lower molecular speeds, but this was neglected in order to maximize the probability of escape. At Chiron's distance at the time of the radiometric observations, less than 84% of the molecules would escape in the ILM case. This percentage decreases by only a few percent at latitudes of ±45°. However, increasing the mass density of Chiron to ρ = 3 g/cm^3 results in less than half of the molecules escaping.

If Chiron is as large and dark as the ILM case allows, but has a large obliquity, then the subsolar latitude could be near the rotational pole by the time Chiron reaches perihelion in 1996. The maximum surface temperature would increase from 77 K to as much as 148 K, and the surface temperature distribution would approach that of the standard thermal model. At this time, the percentage of molecules escaping would be between 70% and 93%, depending on Chiron's density. Thus, the effects of gravity on gas outflow from Chiron may be significant in the ILM case, but diminishes when the surface is best described by the standard thermal model. In the former case, the result that a significant fraction of gas may not escape Chiron's gravitational pull argues that gravitational effects on the dynamical evolution of gas and dust emitted from its surface must be taken into account in detailed models of its coma and atmospheric evolution.

The doubling of the maximum temperature in the above example is due as much to geometry as to the decreasing heliocentric distance. Given the potential for big variations in surface temperature if Chiron has a large obliquity, we suggest that geometry has played and continues to play a critical role in Chiron's activity. This would explain the fact that Chiron was brighter at visual wavelengths in 1978 than in 1983 (*6*).

A large, dark Chiron, having a large obliquity, and a near-equatorial subsolar latitude in 1983, should be increasing dramatically in brightness at thermal wavelengths. Assuming this, and our ILM limits, Chiron might be as much as 100 times brighter at 22.5 μm as it approaches perihelion than it was in 1983. Continued thermal and visual observations of this unusual object and its behavior will provide great insight into the nature of what could be a remnant planetesimal from the outer solar system.

REFERENCES AND NOTES

1. C. T. Kowal, *Int. Astron. Union Cir.* 3129 (1977).
2. B. G. Marsden, *ibid.* 3130 (1977).
3. D. Tholen *et al.*, *ibid.* 4554 (1988).
4. E. Bowell *et al.*, *ibid.* 4579 (1988).
5. S. J. Bus *et al.*, *ibid.* 4684 (1988).
6. S. J. Bus *et al.*, *Icarus* 77, 223 (1989).
7. W. Hartmann *et al.*, *ibid.* **83**, 1 (1990).
8. K. Meech and M. Belton, *Int. Astron. Union Circ.* 4770 (1989).
9. Several comets have been given preliminary asteroid designations initially, their extreme faintness at the time of discovery making the observation of a coma very difficult. In each case (with the exception of Chiron), subsequent astrometric observations have

resulted in the detection of such cometary activity. Chiron's peculiar orbit, however, immediately gave rise to speculation that it may be a comet [C. Kowal, W. Liller, B. Marsden, in *Dynamics of the Solar System*, R. Duncombe, Ed. (Reidel, Dordrecht, 1979), p. 245].
10. K. Meech and M. Belton, *Astron. J.* **100**, 1323 (1990).
11. S. A. Stern, *Publ. Astron. Soc. Pac.* **101**, 126 (1989).
12. M. A'Hearn, H. Campins, D. Schleicher, R. Millis, *Astrophys. J.* **347**, 1155 (1989).
13. R. Millis *et al.*, *ibid.* **324**, 1194 (1988).
14. H. Campins *et al.*, *ibid.* **316**, 847 (1987).
15. R. Sagdeev *et al.*, *Nature* **321**, 262 (1986).
16. H. Keller *et al.*, *ibid.*, p. 320.
17. L. Lebofsky, D. Tholen, G. Rieke, M. Lebofsky, *Icarus* **60**, 532 (1984).
18. L. Lebofsky and J. Spencer, in *Asteroids II*, R. Binzel, T. Gehrels, M. Matthews, Eds. (Univ. of Arizona Press, Tucson, 1989), pp. 128–147.
19. P. Weissman and H. Kieffer, *Icarus* **47**, 302 (1981).
20. M. Sykes *et al.*, *Science* **237**, 1336 (1987).
21. J. Spencer *et al.*, *Icarus* **78**, 337 (1989).
22. J. Spencer, thesis, University of Arizona (1987).
23. M. Belton, in *Comets in the Post-Halley Era*, R. Newburn and J. Rahe, Eds. (Reidel, Amsterdam, in press).
24. P. Thomas, J. Veverka, S. Dermott, in *Satellites*, J. Burns and M. Matthews, Eds. (Univ. of Arizona Press, Tucson, 1986), pp. 802–835.
25. It is interesting to note that were Chiron this elongated, and if it had an obliquity of 90°, the change in light-curve amplitude could be explained by the expected shift in subsolar latitude due to orbital motion over the 4-year interval.
26. *IRAS Explanatory Supplement*, C. A. Beichman *et al.*, Eds. (NASA RP-1190, Washington, DC, 1988).
27. Lebofsky *et al.* (*17*) report a detection at 22.5 μm of 17 ± 9 mJy. This observation used a non-standard "narrow" Q filter, which cut on at +20 μm and off (due to the atmosphere) at ~25 μm (L. Lebofsky, private communication). The effective bandpass of this filter is approximated as a rectangle function in our calculations. The source function used is that of a 4000 K blackbody, corresponding to that of the calibration stars which were used. This reproduces the results of (*17*) to within 1% in diameter and 10% in albedo.
28. E. Bowell *et al.*, in *Asteroids II*, R. Binzel, T. Gehrels, M. Matthews, Eds. (Univ. of Arizona Press, Tucson, 1989), pp. 524–556. In the limit of unit geometric albedo, Chiron's diameter would be 62 km.
29. The diameter is smaller and the albedo larger than the results of Lebofsky *et al.* (*17*), primarily because of a smaller beaming parameter, η, used in the current standard thermal model (*18*).
30. E. Tedesco, D. Matson, G. Veeder, in *Asteroids II*, R. Binzel, T. Gehrels, M. Matthews, Eds. (Univ. of Arizona Press, Tucson, 1989), pp. 290–297.
31. The absolute magnitude, H_V, and slope parameter, G, are taken from (*6*) for 1983, which fell within a period of time when Chiron appeared to be inactive. The thermal phase coefficient, β_E, is used to scale the observed infrared flux to zero phase (*18*). The infrared beaming parameter, η, is used to adjust subsolar temperatures ($T \propto \eta^{-1/4}$) for topographic effects (*18*).
32. We thank M. Schlapfer for his assistance in the reduction of IRAS observations. T. N. Gautier provided some preliminary measurements which resulted in the eventual undertaking of the current work. We also thank the scientific support staff of the Infrared Processing and Analysis Center for their helpfulness. M. Belton provided many thoughtful and useful comments in his review of a manuscript draft. The final manuscript benefited greatly from reviews by E. Bowell and P. Weissman. D. Davis and S. J. Bus are thanked for useful information and discussions. This work was supported in part by Mission Research Corporation Contract SC-0014-88-0002, NASA Grant NAG5-1370, and the Jamieson Science and Engineering Internal Research and Development Program.

1 October 1990; accepted 3 January 1991

A-Axis–Oriented $YBa_2Cu_3O_7/PrBa_2Cu_3O_7$ Superlattices

C. B. Eom,* A. F. Marshall, J.-M. Triscone,† B. Wilkens, S. S. Laderman, T. H. Geballe

A modulated structure has been fabricated from high transition temperature superconductors where the individual CuO_2 planes are composed of alternating superconducting and insulating strips. This structure is made by growing *a*-axis–oriented $YBa_2Cu_3O_7/PrBa_2Cu_3O_7$ superlattices by 90° off-axis sputtering on (100)$SrTiO_3$ and (100)$LaAlO_3$ substrates. Superlattice modulation is observed to a modulation wavelength of 24 angstroms (12 angstroms–$YBa_2Cu_3O_7$/12 angstroms–$PrBa_2Cu_3O_7$), both by x-ray diffraction and by cross-sectional transmission electron microscopy. Rutherford backscattering spectroscopy indicates a high degree of crystalline perfection with a channeling minimum yield of 3 percent. Quasi–one-dimensional conductivity should be obtainable in these structures.

The study of high transition-temperature (T_c) superconductor (HTS) heterostructures is motivated not only by the need to fabricate sandwich-type tunnel junctions but also because artificial structures can be valuable model systems for investigating particular physical properties. In the so-called "123" structure and among many possible systems, $YBa_2Cu_3O_7$ (YBCO) and $PrBa_2Cu_3O_7$ (PBCO) make a good combination because of their shared 123 structure and close lattice match and the fact that PBCO is an insulator, in contrast to superconducting YBCO. Additionally, the electrical properties of $Pr_{1-x}Y_xBa_2Cu_3O_7$ can be varied from insulator to superconductor by increasing the Y concentration.

Epitaxial growth of *c*-axis–oriented PBCO on YBCO layers was first reported by Poppe *et al.* (*1*). Shortly after their work, Triscone *et al.* (*2, 3*) demonstrated the growth of *c*-axis–oriented YBCO/DyBCO and YBCO/PBCO superlattices down to a 24 Å modulation wavelength Λ (Λ is the sum of the individual thicknesses in the superlattice). Other groups (*4, 5*) have also succeeded in fabricating *c*-axis YBCO/PBCO superlattices and have studied their superconducting properties.

From a scientific and technological point of view the growth of *a*-axis films and multilayers is very attractive. This is so because the larger *ab*-plane superconducting coherence length should produce a stronger proximity effect in *a*-axis superlattices and superior sandwich-type tunnel junctions, which have yet to be made in any high T_c cuprate superconductors. Further, the *a*-axis superlattice mismatch at the YBCO/PBCO interface is significantly smaller than the interface mismatch for *c*-axis superlattices.

Owing to the change in process conditions required to form *a*-axis–oriented YBCO as well as anisotropies in atomic diffusivities and crystal growth rates for the layered perovskites, it is a priori unclear whether fine-scale multilayer *a*-axis structures can be synthesized. We report here that modulated *a*-axis structures with modulation wavelengths down to 24 Å can be made with a high degree of structural order and extremely smooth surfaces to thicknesses of at least 4800 Å, that is with 200 interfaces.

Figure 1 is a schematic diagram of the unit cell of an ideal 12 Å–YBCO/12 Å–PBCO *a*-axis multilayer. Theoretically, it is possible to grow *a*-axis structures with an 8 Å modulation wavelength. The minimum *c*-axis superlattice modulation wavelength is 24 Å, corresponding to the fact that the *c*-axis is about three times larger than the *a*-axis. An interesting feature of *a*-axis heterostructure can be seen in Fig. 1: the CuO_2 planes are vertical and the very same CuO_2 plane can be locally superconducting or insulating in strips, the width of which is one-half of the superlattice period, depending on whether the rare earth neighbors of the plane are Y or Pr. This property permits, by decreasing the YBCO width, a modification of the dimensionality of the system. A change from quasi–two-dimensional (2D) behavior to quasi–one-dimensional (1D) behavior is expected as the YBCO layer width, d_s, is decreased down to the coherence length in the *ab* plane ξ_{ab} and, for well-chosen material parameters, a crossover from quasi-1D to quasi-2D behavior is expected at a temperature T^* below T_c at which ξ_{ab} becomes less than d_s.

We recently reported the synthesis and

C. B. Eom, J.-M. Triscone, T. H. Geballe, Department of Applied Physics, Stanford University, Stanford, CA 94305.
A. F. Marshall, Center for Materials Research, Stanford University, Stanford, CA 94305.
B. Wilkens, Bellcore, Red Bank, NJ 07701.
S. S. Laderman, Hewlett-Packard Co., Palo Alto, CA 94304.

*Also at the Center for Materials Research, Stanford University, Stanford, CA 94305.
†On leave from the University of Geneva, DPMC, 1211 Geneva 4, Switzerland.